

Fabrication of $\text{BaCe}_{0.8}\text{Y}_{0.2}\text{O}_3$ dense film on perovskite-type oxide electrode substrates

Makiko Asamoto, Hirono Shirai, Hiroyuki Yamaura,
Hidenori Yahiro*

Department of Materials Science and Biotechnology, Graduate School of Science and Engineering, Ehime University, Matsuyama 790-8577, Japan

Available online 19 March 2007

Abstract

The electrochemical performances were investigated for proton-conducting solid oxide fuel cells (SOFCs) with the perovskite-type oxide cathodes. As for proton-conducting SOFC using $\text{BaCe}_{0.8}\text{Y}_{0.2}\text{O}_3$ (BCYO) and $\text{SrCe}_{0.95}\text{Yb}_{0.05}\text{O}_3$ (SCYO) electrolytes, $\text{La}_{0.7}\text{Sr}_{0.3}\text{FeO}_3$ (LSFO) cathode showed the best electrochemical performance among the perovskite-type oxides tested in the present study. The spin-coating technique was applied to fabricate BCYO thin film on the LSFO substrate. With this technique, dense and crack-free BCYO thin film could be fabricated on LSFO electrode substrate. However, the electrical conductivity of BCYO thin film fabricated on LSFO electrode substrate was lower than that of the bulk BCYO specimen, suggesting the formation of the second phase between the electrolyte film and the oxide substrate.

© 2007 Elsevier Ltd. All rights reserved.

Keywords: Films; Electrical conductivity; Perovskites; Fuel cells; Substrate

1. Introduction

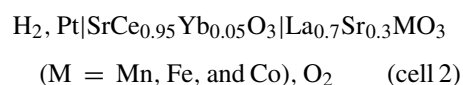
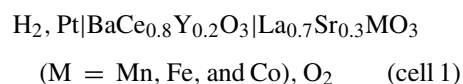
Several doped perovskite-type oxides such as Yb-doped SrCeO_3 ¹ and Nd-, Y-, or Gd-doped BaCeO_3 ^{2,3} showed high protonic conductivities and are of interest for application in SOFCs.^{4–6} Iwahara and co-workers⁶ reported the operation of a H_2 – O_2 fuel cell using SCYO solid electrolyte at 1073–1273 K. However, they pointed out that the cathode overpotential is high similar to that observed for SOFCs with an oxide-ion conductor. Recently, we have demonstrated that the cathodic overpotential of LSFO was smaller than that of a platinum electrode for proton-conducting SOFC.⁷

In this paper, the results of structure and electrical conductivity measurements of BCYO thin film fabricated on LSFO electrode substrate are presented. Several techniques such as MOCVD,⁸ a polymeric precursor spin-coating,⁹ and a colloidal suspension spin-coating,¹⁰ have been reported for preparing thin film of proton conductors. Spin-coating is one of the simplest techniques among the techniques reported for developing thin film electrolytes and with this technique, dense and crack-free YSZ films supported on NiO-SDC substrates were attained after sintering at 1573 K for 5 h.¹¹ Therefore, we attempted to fabri-

cate a thin film on LSFO electrode substrate by spin-coating suspensions of BCYO powders.

2. Experimental

Cathode materials ($\text{La}_{0.7}\text{Sr}_{0.3}\text{FeO}_3$, $\text{La}_{0.7}\text{Sr}_{0.3}\text{MnO}_3$, and $\text{La}_{0.7}\text{Sr}_{0.3}\text{CoO}_3$) and electrolytes (SCYO and BCYO) were prepared by solid-state reaction reported elsewhere.⁷ XRD measurement (Rigaku, RINT2200HF) demonstrated that the obtained samples exhibited single-phase XRD patterns. The electrochemical data were collected by the following two fuel cells;



where the diameter and the thickness of disc electrolyte were ca. 9 mm and ca. 2.3 mm, respectively, and the sputtered Pt was used as an anode. The thickness of cathode was confirmed by scanning electron microscopy (JEOL, JSL-5310) to be around 0.2 mm.

* Corresponding author. Tel.: +81 89 927 9929; fax: +81 89 927 9946.
E-mail address: hyahiro@eng.ehime-u.ac.jp (H. Yahiro).

The LSFO electrode substrate was prepared by the solid-state reaction. La_2O_3 (99.99%, Wako), SrCO_3 (95%, Wako), and Fe_2O_3 (99.5%, Wako) were mixed in appropriate ratio and calcined at 1673 K for 10 h in air. The powder sample was uniaxially pressed into pellets under a pressure of 2000 kg cm^{-2} and then heated at 1673 K for 10 h in air.

Polycrystalline BCYO precursor powders for spin-coating were prepared by the following evaporation-to-dryness method. $\text{Ba}(\text{CH}_3\text{COO})_2$ (99%, Wako), $\text{Ce}(\text{NO}_3)_3 \cdot 6\text{H}_2\text{O}$ (98%, Wako), and $\text{Y}(\text{NO}_3)_3 \cdot 6\text{H}_2\text{O}$ (99.99%, Kanto Chemical) with an appropriate ratio were dissolved in deionized water and heated under stirring until the water was completely vaporized. The obtained solid products were calcined at 1273 K for 10 h to yield the BCYO precursor powders, of which the crystalline structure was confirmed by XRD measurement. The BCYO powder was ultrasonically mixed with isopropanol for 60 min to form a homogeneous dispersion. The BCYO powder-suspended solution was added dropwise onto a LSFO substrate rotated at 7200 rpm. The sample was dried at room temperature and annealed at 1473–1573 K for 12 h. The coating-drying-annealing cycles were repeated several times. Here-in-after, the samples were abbreviated as BCYO/LSFO(1573, 3), where the numerical values in the parenthesis indicate the annealing temperature and the number of cycles.

The electrical conductivities of BCYO thin films were studied by a conventional 2-probe ac measurement with LCR meter (Ando, type AG-4311). The impedance spectra were obtained with the frequency range of 0.1–100 kHz at 873–1073 K.

3. Results and discussion

3.1. Properties of proton-conducting SOFC with the different cathode

The electrochemical data of two cells, cells 1 and 2, are shown in Fig. 1. In both cases, when LSFO was used as a cathode, a large current density was obtained at 773 K. From these results, it was concluded that among the various perovskite-type oxide examined, LSFO is the most suitable potential candidate for the cathode material in a H_2 – O_2 fuel cell with a proton conductor.

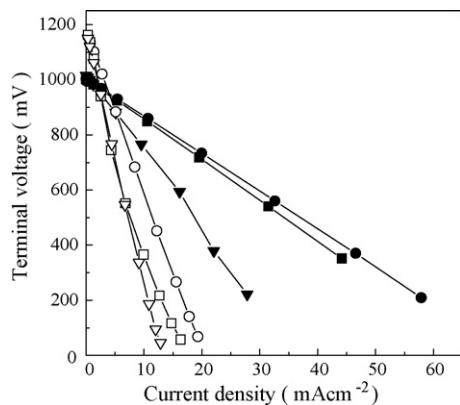


Fig. 1. I - V characteristics of (■, ●, ▼) cell 1 and (□, ○, ▽) cell 2 at 973 K. Cathode: (■, □) $\text{La}_{0.7}\text{Sr}_{0.3}\text{MnO}_3$, (●, ○) $\text{La}_{0.7}\text{Sr}_{0.3}\text{FeO}_3$, and (▼, ▽) $\text{La}_{0.7}\text{Sr}_{0.3}\text{CoO}_3$.

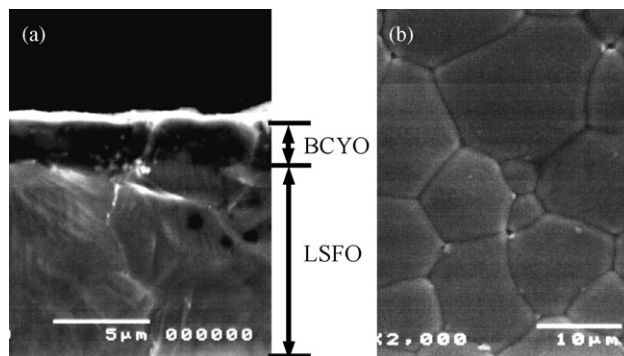


Fig. 2. SEM images of (a) the cross-section and (b) the surface of BCYO/LSFO(1573, 3) device.

Therefore, LSFO was used as a cathode material in subsequent measurements.

3.2. Structure of BCYO/LSFO device

Fig. 2 shows SEM micrographs of cross-section and surface of BCYO/LSFO(1573, 3) device. As can be seen in Fig. 2(a), dense and crack-free BCYO thin film was obtained with thickness of about $1.7 \mu\text{m}$. The thicknesses of BCYO/LSFO(1573, 1) and BCYO/LSFO(1573, 7) devices were measured by similar SEM measurements to be 0.5 and $4.8 \mu\text{m}$, respectively. This result indicates that the thickness of BCYO thin film is proportional to the number of spin-coating cycles. Fig. 2(b) shows a SEM micrograph of the surface morphology of the BCYO/LSFO(1573, 3) device. The grain size is relatively large, suggesting that the BCYO thin films grew with preferred crystallographic orientation on the surface LSFO substrate.

Fig. 3(a) presents the XRD pattern of BCYO/LSFO(1573, 3). A weak peak assigned to BCYO was observed at $2\theta = 28.7^\circ$ together with a set of peaks assigned to the LSFO substrate. This result demonstrated the successful preparation of BCYO thin film on LSFO electrode substrate. The increase in the number of cycles resulted in both an increment of XRD peak intensity

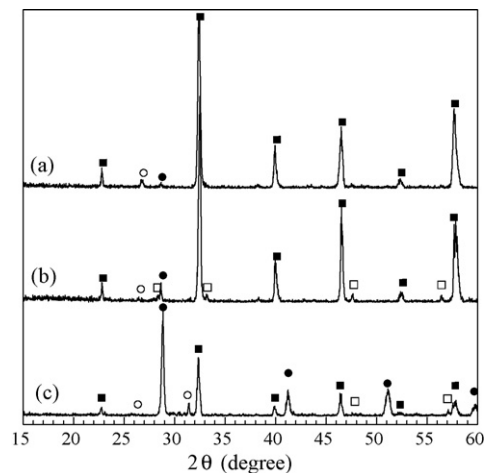


Fig. 3. XRD patterns of (a) BCYO/LSFO(1573, 3), (b) BCYO/LSFO(1573, 7), and (c) the 50/50vol% BCYO/LSFO mixed powder annealed at 1573 K. (●) BCYO, (■) LSFO, (○) BaFeO_3 , and (□) CeO_2 .

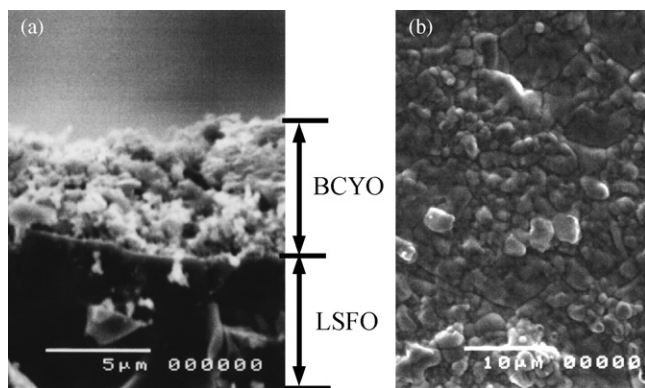


Fig. 4. SEM images of (a) the cross-section and (b) the surface of BCYO/LSFO(1473, 3) device.

of BCYO and the appearance of new XRD peaks, as shown in Fig. 3(b). The details of these new peaks will be discussed later.

Fig. 4 shows SEM micrographs of the cross-section and the surface morphology of the BCYO/LSFO(1473, 3) device annealed at lower temperature. In contrast to BCYO/LSFO(1573, 3), the thin film of BCYO/LSFO(1473, 3) device does not appear to be dense although the XRD peak assigned to BCYO was clearly observed. This indicates that the BCYO thin film growth rate on LSFO substrate was very slow at 1473 K.

3.3. Electrical conductivities of BCYO/LSFO devices

The electrical conductivities of BCYO/LSFO(1573, 3) and BCYO/LSFO(1573, 7) devices are shown in Fig. 5 as a function of reciprocal temperature. The electrical conductivity for the bulk polycrystalline BCYO is also shown in this figure. The electrical conductivity of bulk BCYO is about 1 and 2 orders of magnitude larger than those of BCYO/LSFO(1573, 3) and BCYO/LSFO(1573, 7), respectively. This suggests that there is the large interfacial resistance between a BCYO thin film and LSFO electrode substrate due to the formation of the second

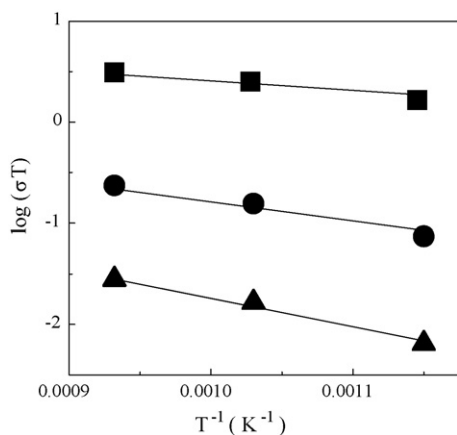


Fig. 5. Electrical conductivities of (●) BCYO/LSFO(1573, 3), (▲) BCYO/LSFO(1573, 7), and (■) disc BCYO as a function of reciprocal temperature.

phase with low electrical conductivity, because the electrical conductivity of LSFO was much higher than that of BCYO.

Diffusion of metal ions leading to the chemical reaction at the electrode and electrolyte interface also causes degradation of the electrical properties. LaCoO₃ and LaMnO₃ were reported to react with YSZ to yield the poorly conducting La- and Sr-zirconate at the interface,^{12,13} whereas LSFO is thermally stable in contact with YSZ at 1673 K.¹⁴

In order to presume the formation of the second phase at electrolyte/electrode substrate interface, the XRD measurement was carried out for the 50/50 vol% BCYO/LSFO mixed powder annealed at 1573 K for 12 h. The XRD pattern is shown in Fig. 3(c). Besides the sets of peaks assigned to BCYO and LSFO, new peaks were observed at 26.3°, 31.5°, 47.5°, and 56.3°. The peaks at 26.3 and 31.5° could be assigned to BaFeO₃ (JSPDS file no. 23-1024), while the peaks at 47.5° and 56.3° could be assigned to CeO₂ (JSPDS file no. 34-394). Such second phases may be formed at electrolyte/electrode substrate interface, resulting in the decrease in the electrical conductivity.

The linear relationship between log electrical conductivity and reciprocal temperature was obtained for all samples, suggesting that the activation energy of electrical conduction remains unchanged in the temperature range of 873–1073 K. The activation energies were determined from the slope of each line to be 26.6, 45.3, and 57.3 kJ mol⁻¹ for bulk BCYO, BCYO/LSFO(1573, 3), and BCYO/LSFO(1573, 7), respectively. The fact that the activation energies of BCYO/LSFO were higher than that of BCYO also suggests the presence of the interfacial effect. Further studies to inhibit the chemical reaction between the dense thin film and the oxide substrate are in progress.

4. Conclusion

The following aspects were obtained from the present study.

- (1) When LSFO was used as a cathode, the best electrochemical performance was obtained for proton-conducting SOFCs.
- (2) With the present spin-coating technique, dense and crack-free BCYO thin film on LSFO electrode substrate was attained after annealing at 1573 K.
- (3) The electrical conductivity of BCYO fabricated on LSFO electrode substrate was lower than that of the bulk BCYO.

Acknowledgements

This work was supported in part by the Core Research for Evolutional Science and Technology (CREST) program of the Japan Science and Technology Agency (JST).

References

1. Iwahara, H., Esaka, T., Uchida, H. and Maeda, N., Proton conduction in sintered oxides and its application to steam electrolysis for hydrogen production. *Solid State Ionics*, 1981, **3/4**, 359–363.
2. Liu, J. F. and Bowick, A. S., The incorporation and migration of protons in Nd-doped BaCeO₃. *Solid State Ionics*, 1992, **50**, 131–138.

3. Iwahara, H., Uchida, H., Ono, K. and Ogaki, K., Proton conduction in sintered oxides based on BaCeO_3 . *J. Electrochem. Soc.*, 1988, **135**, 529–533.
4. Iwahara, H., Uchida, H. and Maeda, M., High temperature fuel and steam electrolysis cells using proton conductive solid electrolytes. *J. Power Sources*, 1982, **7**, 293–301.
5. Bonanos, N., Ellis, B. and Mahmood, M. N., Construction and operation of fuel cells based on the solid electrolyte $\text{BaCeO}_3\text{:Gd}$. *Solid State Ionics*, 1991, **44**, 305–311.
6. Uchida, H., Tanaka, S. and Iwahara, H., Polarization at Pt electrodes of a fuel cell with a high temperature-type proton conductive solid electrolyte. *J. Appl. Electrochem.*, 1985, **15**, 93–97.
7. Yamaura, H., Ikuta, T., Yahiro, H. and Okada, G., Cathodic polarization of strontium-doped lanthanum ferrite in proton-conducting solid oxide fuel cell. *Solid State Ionics*, 2005, **176**, 269–274.
8. Pan, M., Meng, G. Y., Chen, C. S., Peng, D. K. and Lin, Y. S., MOCVD synthesis of yttria doped perovskite type SrCeO_3 thin films. *Mater. Lett.*, 1998, **36**, 44–47.
9. Kosacki, I. and Anderson, H. U., The structure and electrical properties of $\text{SrCe}_{0.95}\text{Yb}_{0.05}\text{O}_3$ thin film protonic conductors. *Solid State Ionics*, 1997, **97**, 429–436.
10. Hamakawa, S., Li, L., Li, A. and Iglesia, E., Synthesis and hydrogen permeation properties of membranes based on dense $\text{SrCe}_{0.95}\text{Yb}_{0.05}\text{O}_{3-\alpha}$ thin films. *Solid State Ionics*, 2002, **48**, 71–81.
11. Xu, X., Xia, C., Huang, S. and Peng, D., YSZ thin films deposited by spin-coating for IT-SOFCs. *Ceram. Int.*, 2005, **31**, 1061–1064.
12. Takeda, Y., Kanno, R., Noda, M., Tomida, Y. and Yamamoto, O., Cathodic polarization phenomena of perovskite oxide electrodes with stabilized zirconia. *J. Electrochem. Soc.*, 1987, **134**, 2656–2661.
13. Figueiredo, F. M., Labrincha, J. A., Frade, J. R. and Marques, F. M. B., Reactions between a zirconia-based electrolyte and LaCoO_3 -based electrode materials. *Solid State Ionics*, 1997, **101–103**, 343–349.
14. Simner, S. P., Shelton, J. P., Anderson, M. D. and Stevenson, J. W., Interaction between $\text{La}(\text{Sr})\text{FeO}_3$ SOFC cathode and YSZ electrolyte. *Solid State Ionics*, 2003, **161**, 11–18.